J. Fluid Mech. (1977), *vol.* 81, *part* 2, *pp.* 295–304
Printed in Great Britain

Numerical computation of Taylor vortices

By A. K. MAJUMDAR AND D. BRIAN SPALDING
Department of Mechanical Engineering, Imperial College, London

(Received 26 October 1976)

A finite-difference procedure for three-dimensional parabolic flows is used to predict the development of Taylor vortices in the flow between concentric rotating cylinders, resulting from the growth of small disturbances of a Couette flow. Predictions of such flows are presented in the developing and fully developed region. A precise calculation of the wavelength of the vortices has been possible by employing a periodic boundary condition on the pressure field. The predicted torque coefficient compares well with experimental data. The critical Taylor number has also been predicted with good accuracy.

1. Introduction

1.1. *The problem considered*

The phenomenon of Taylor vortices is of significance to the understanding of hydrodynamic stability of fluid flows. Taylor (1923) observed the generation of a system of toroidal vortices in flows between long rotating concentric cylinders (figure 1). In his experiment, the inner cylinder rotated while the outer was at rest. These vortices, now known as Taylor vortices, occur if a certain parameter exceeds a critical value; this is the Taylor number ($T \equiv w_p d\nu^{-1}(d/R_i)^{\frac{1}{2}}$, where d denotes the width of the annular gap, R_i the inner radius, w_p the peripheral velocity of the inner cylinder and ν the kinematic viscosity of the fluid). The formation of these vortices can be explained by the fact that if a rotating fluid particle is displaced radially outwards by some means then it tends to move further outwards because the 'centrifugal force' on it exceeds that on the less rapidly rotating fluid around it.

In the present study, the parabolic differential equations governing developing three-dimensional duct flows are solved by the procedure of Patankar & Spalding (1972) to predict the critical Taylor number and the development of the vortices.

1.2. *Previous work*

The flow between concentric rotating cylinders has been subjected to both experimental and theoretical investigations for many years. In this subsection, an outline is given of the previous work.

Experimental. The early experimental investigations of Couette (1890) and Mallock (1888) were directed towards testing the validity of the Newtonian-stress approximation in the Navier–Stokes equation. In Couette's experiment, the inner cylinder was fixed and the outer one was rotating. It was found that the drag on the inner cylinder was proportional to the velocity of the outer one until a certain critical velocity was reached. With a further increase of speed, the drag increased at a rate greater than

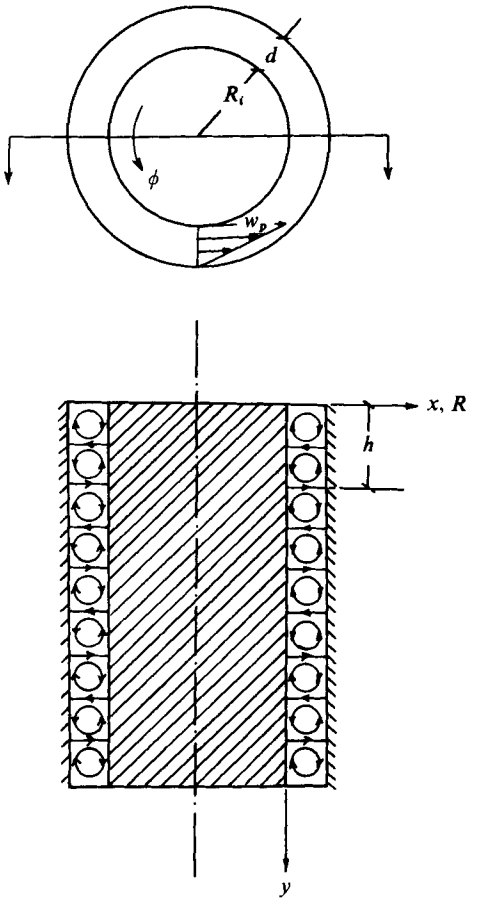

FIGURE 1. Physical situation and co-ordinate system.

the rate of increase of the cylinder velocity. This phenomenon was attributed to the onset of turbulence. Mallock extended this experiment to cover the case in which the inner cylinder rotated and the outer one remained at rest. These experiments indicated a very low critical speed for the transition of the flow. In a later investigation, Taylor (1923) discovered the existence of toroidal vortices above the critical speed. Taylor (1936) also measured torque–velocity characteristics.

An extensive investigation of such flows, using flow-visualization techniques, was carried out by Coles (1965). He identified two distinct kinds of transition in flow between concentric cylinders. The first, stable vortex flows are established when the velocity of the inner cylinder is increased to a value just above the critical Taylor number. The vortices are closed rings wrapped around the inner cylinder. This flow has been observed to be two-dimensional. As the velocity is further increased beyond the critical Taylor number, the flow pattern changes in character and becomes three-dimensional. It was not possible to locate precisely the Taylor number at which the three-dimensional effects become prominent, but Coles reported a zone of hysteresis near the second transition. The three-dimensional motion consists of a circumferential wave motion, superimposed on the cellular structure observed after the first transition.

Theoretical. The stability of flow between concentric rotating cylinders was first investigated by Rayleigh (1916), who assumed that the fluid was inviscid. The case of viscous fluid was first investigated by Taylor (1935) by means of a linear theory. Later Stuart (1958) investigated the problem, retaining the nonlinear terms in the equation of motion. He discovered the existence of equilibrium between the transfer of energy from the base flow to the secondary flow and the viscous energy dissipation in the secondary flow. A further extension of such concepts was carried out by Davey (1962). Recently Taylor-vortex flow between eccentric cylinders has been the subject of theoretical investigations by DiPrima & Stuart (1972, 1975). Meyer (1966) investigated numerically the fully developed situation by an explicit two-dimensional time-marching method.

1.3. *Present contribution*

The present study concerns the numerical prediction of the development of Taylor vortices when the laminar Couette flow is slightly disturbed; the finite-difference method of Patankar & Spalding (1972) is used to compute the developing and fully developed flow fields.

The axial length of the vortices is determined by employing a periodic boundary condition on the pressure field. The drag characteristics are compared with the experimental results of Taylor (1936). The critical Taylor number is predicted to a good accuracy.

In the present investigation, the computations are performed for moderate Taylor numbers ($T < 55$), because it is only for these that the flow is two-dimensional, as explained above. The fluid properties are taken as uniform.

2. Theory

2.1. *The geometry in question*

In a strict sense, the flow system to be studied is incapable of realization. A wide duct with concentric cylindrical walls in which the main direction of flow is circumferential is considered. This duct is imagined to have an entrance, where the circumferential velocity is linear with radius, and to extend *infinitely far* in the downstream (ϕ) direction. It is the words in italics which express the impossible feature, because ϕ cannot exceed 2π without interference. However, computer programs are not subject to such practical limitations.

2.2. *Differential equations*

The physical situation illustrated in figure 1 may conveniently be described in the x, y, ϕ co-ordinate system. The governing differential equations are as follows if viscous transport in the ϕ direction is neglected.

x momentum:

$$\rho\left(u\frac{\partial u}{\partial x}+v\frac{\partial u}{\partial y}+\frac{w}{R}\frac{\partial u}{\partial \phi}-\frac{w^2}{R}\right)=-\frac{\partial p}{\partial x}+\frac{\partial \tau_{xx}}{\partial x}+\frac{\partial \tau_{xy}}{\partial y}+\frac{\tau_{xx}}{R}. \tag{1}$$

y momentum:

$$\rho\left(u\frac{\partial v}{\partial x}+v\frac{\partial v}{\partial y}+\frac{w}{R}\frac{\partial v}{\partial \phi}\right)=-\frac{\partial p}{\partial y}+\frac{\partial \tau_{yx}}{\partial x}+\frac{\partial \tau_{yy}}{\partial y}+\frac{\tau_{yx}}{R}. \tag{2}$$

ϕ momentum:

$$\rho\left(u\frac{\partial w}{\partial x}+\frac{uw}{R}+v\frac{\partial w}{\partial y}\frac{w}{R}\frac{\partial w}{\partial \phi}\right)=-\frac{\partial \bar{p}}{R\partial\phi}+\frac{\partial \tau_{\phi x}}{\partial x}+\frac{\partial \tau_{\phi y}}{\partial y}+\frac{2}{R}\tau_{\phi x}. \tag{3}$$

Continuity:

$$\frac{\partial u}{\partial x}+\frac{\partial v}{\partial y}+\frac{1}{R}\frac{\partial w}{\partial \phi}+\frac{u}{R}=0. \tag{4}$$

In these equations, u, v and w represent the velocity components in the x, y and ϕ co-ordinate directions respectively. ρ represents the density and p is the pressure field. The τ's represent shear stresses and are expressible in terms of the velocity gradients and the kinematic viscosity, which is presumed to be uniform.

A feature of these equations which deserves especial note is that a single pressure $\bar{p}$ is supposed to prevail at each cross-section in the ϕ momentum equation (3), but in the x and y momentum equations (1) and (2) the pressure p is allowed to vary over the cross-section. This is an expression of the 'pressure uncoupling' that is characteristic of parabolic flows (Patankar & Spalding 1972). It does not lead to any significant error when the fully developed situation is reached. It should be noted that dependency of the velocity field on ϕ ceases in a fully developed situation: the flow becomes two-dimensional.

2.3. *Boundary conditions*

A radially linear w velocity profile, together with a perturbation whose magnitude was 5 % of the mean value, was set as the upstream condition. The radial (u) and axial (v) components were assumed to be zero.

The boundary conditions on the cylinder walls are

$$u=v=0, \quad w=R_i\,\Omega \quad \text{at the inner wall,}$$

where R_i is the radius of the inner cylinder and Ω its angular velocity, and

$$u=v=w=0 \quad \text{at the outer wall.}$$

However, at boundaries normal to the cylinder axis it is necessary to satisfy a *periodic* boundary condition: the pressure difference across the integration domain, which has been required to consist of two vortices, must be zero at all radii. This condition can be implemented only when the correct width of the vortices has been found. The search for the correct width is a special feature of the problem; it has been accomplished by an iterative procedure, described in the following subsection.

2.4. *Solution procedure*

The differential equations described in § 2.1 have been solved by the method of Patankar & Spalding (1972) embodied in the computer code STABLE (*S*teady *T*hree-dimensional *A*nalyser of *B*oundary *L*ayer *E*quations). A marching-integration technique is employed in the circumferential (ϕ) direction in which, at each cross-section of the annulus passage, a two-dimensional field of variables is determined. A complete description of the method has been given by Patankar & Spalding (1972); in the present context, it takes the following form.

(1) The axial width of the integration domain is guessed.

(2) The pressure distribution $p(x, y)$ at a longitudinal station and the average pressure $\bar{p}$ at a station downstream of it are guessed.

(3) The momentum equations for the x, y and ϕ directions are then solved to get a first approximation to the velocity distribution.

(4) The mean pressure $\bar{p}$ at the downstream station is kept the same as that at the upstream station by adjusting the mass flow rate through the integration domain. The mass flow rate is adjusted by reference to the longitudinal (ϕ) momentum equation and the boundary conditions.

(5) Since the cross-stream velocities u and v do not satisfy the continuity equation locally, a 'Poisson' equation for the pressure is derived from this equation and from the two momentum equations; this 'Poisson' equation is then solved for corrections to the pressure field p. Then the cross-stream velocities are corrected accordingly.

(6) A new downstream station is chosen and steps 2–5 are repeated.

(7) Steps 2–6 are repeated until an unchanging flow pattern has developed.

(8) A test is made to ensure that the integrated pressure difference across the boundaries in the axial direction is less than a pre-specified small quantity; if not, steps 1–7 are repeated with a different width (axial extent) of the integration domain.

3. Results

3.1. *Computational details*

In the majority of computations from which the following results were derived, the finite-difference grid possessed 11 intervals in the radial and axial directions. The computations were shown by experimentation with finer and coarser grids to depend little on grid fineness. The results of such tests are shown in figure 2.

The forward-step dependency was tested by repeating the computations with smaller and larger step sizes; a step size was then chosen which was small enough not significantly to affect the solution. The computer time needed to perform one fully developed computation was of the order of 250s on a CDC6600 computer, for 1000 forward steps.

3.2. *Axial width of vortices*

The technique adopted to determine the correct width of the vortices has already been explained in § 2.3. Figure 3 represents the variation of the non-dimensional pressure with the non-dimensional axial width of the integration domain; each point represents the result of a different integration process. A zero pressure difference was never precisely attained; but an h/D of 1·875 was taken as being the correct one in the example shown.

3.3. *Flow field*

In this subsection the results for developing and fully developed flow are presented. Figure 4 represents the development of the circumferential, radial and axial velocities from a perturbed one-dimensional solution (at $\phi = 0$). Figures 5 (a) and (b) show the velocity vectors representing the secondary flow field in a fully developed situation at two different Taylor numbers. The circumferential velocity and pressure fields for these two situations are plotted in figures 6 and 7.

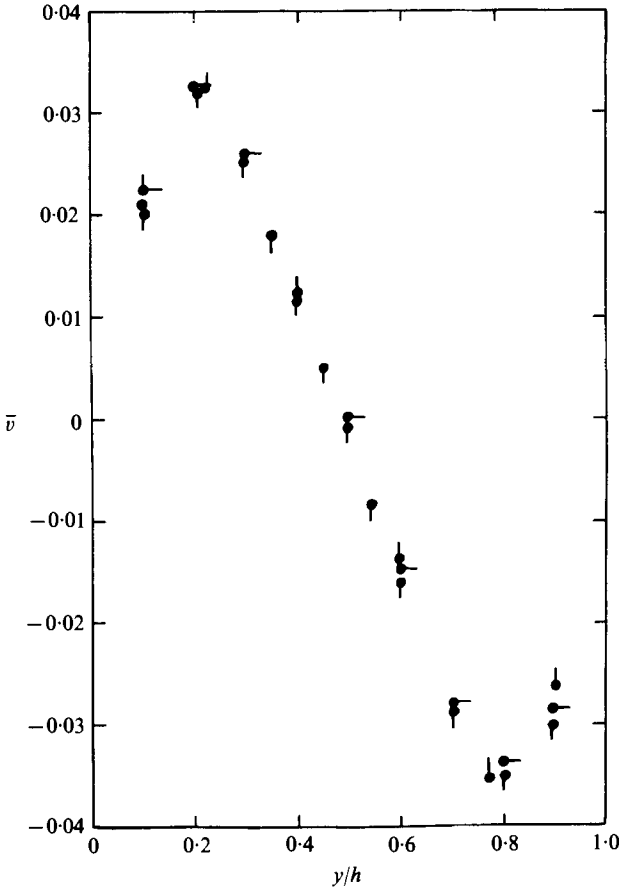

FIGURE 2. Effect of grid size on axial-velocity distribution $\bar{v} \equiv v/w_p$, where w_p is the peripheral velocity of the inner cylinder. ●, 9 × 9 grid; ●, 12 × 12 grid; ●, 15 × 15 grid. $x/d = 0{\cdot}85$.

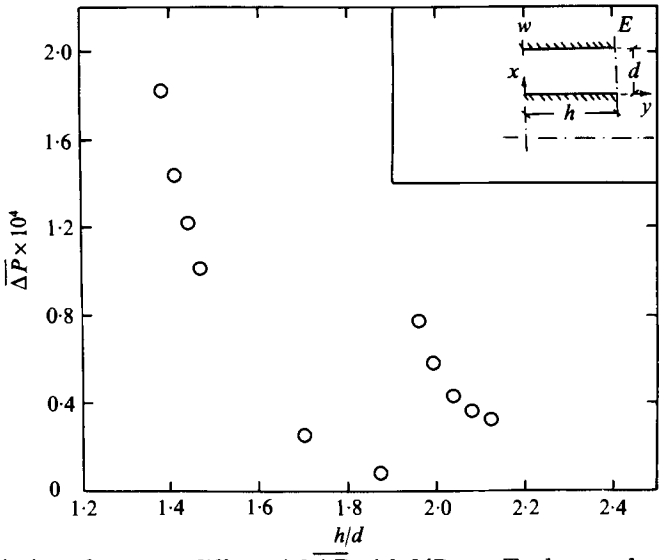

FIGURE 3. Variation of pressure differential $\overline{\Delta P}$ with h/D at a Taylor number of 45; ΔP is defined (see inset sketch) by

$$\overline{\Delta P} \equiv \frac{1}{d}\int_0^d \frac{|p_w - p_E|\,dx}{\frac{1}{2}\rho \bar{w}_p^2}.$$

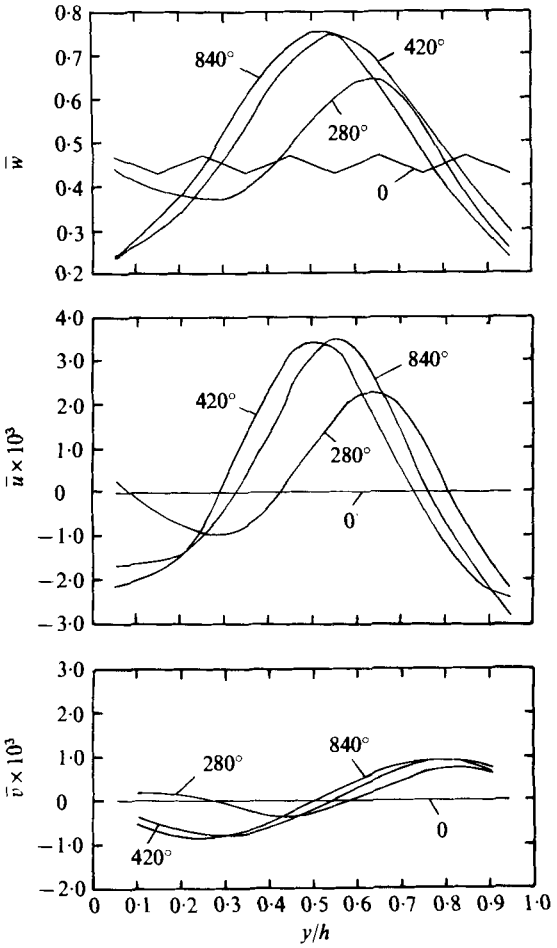

FIGURE 4. Development of circumferential ($\bar{w} = w/w_p$), radial ($\bar{u} \equiv u/w_p$) and axial ($\bar{v} \equiv v/w_p$) velocity distribution at a Taylor number of 55; $x/d = 0{\cdot}45$, $\phi = 0$, 280°, 420° and 840°.

3.4. *Drag characteristics*

Figure 8 compares the predictions of the torque coefficient with the measurements of Taylor (1936). The torque coefficient C_M is defined as

$$C_M \equiv M_i/\tfrac{1}{2}\pi\rho w_p^2 R_i^2 h, \tag{5}$$

where M_i is the torque required to rotate the inner cylinder. Good agreement is observed between numerical predictions and measurements, in the region studied. The Taylor number at which vortices start, i.e. 41, has been located fairly well.

4. Discussion

The results described in § 3 demonstrate that it has been possible to make a prediction of the detailed flow structure of Taylor vortices which is in qualitative and quantitative agreement with such experimental data as exist for the two-dimensional regime. However no effort has been made to perform computations at high Taylor numbers, at which the flow develops a wavy form (Coles 1965), for it seems certain

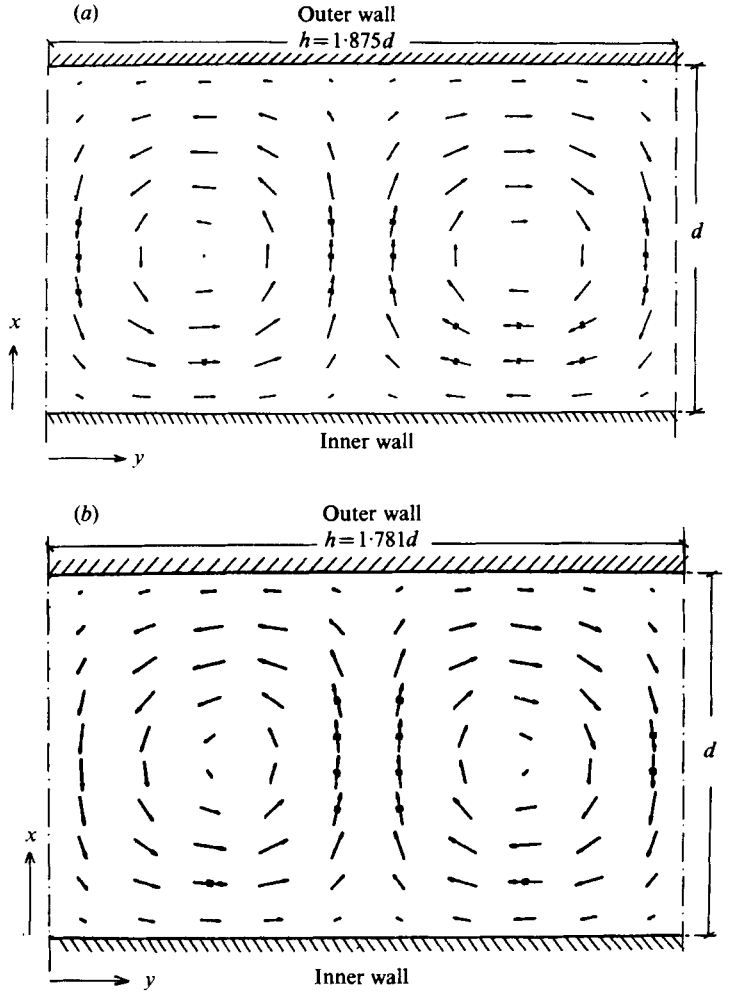

FIGURE 5. Secondary flow field at a Taylor number of (*a*) 45 and (*b*) 55.

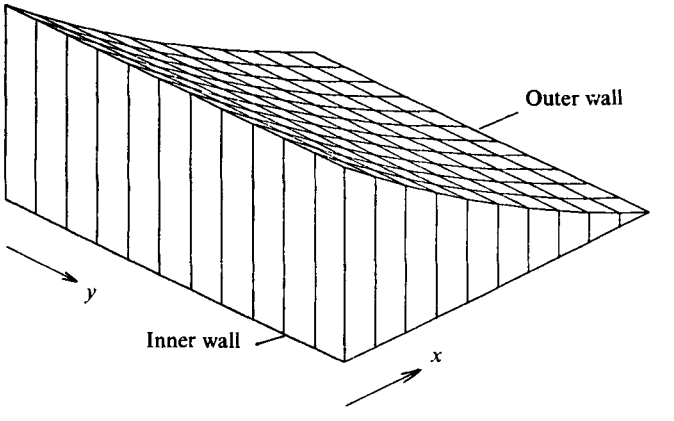

FIGURE 6 (*a*). For legend see facing page.

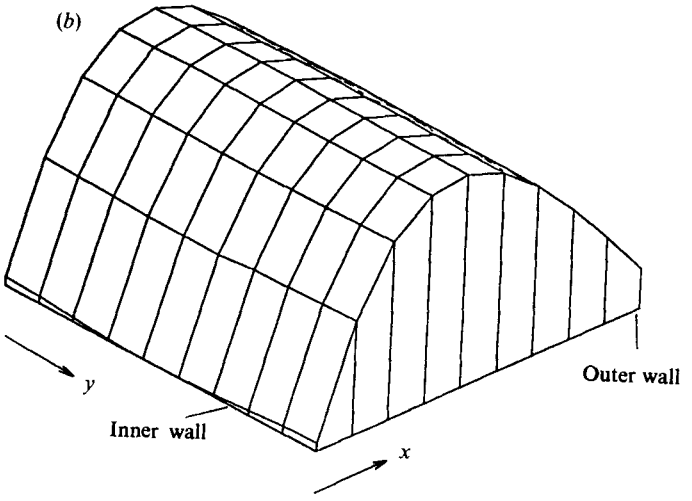

FIGURE 6. (*a*) Circumferential velocity ($\bar{w} = w/w_p$) distribution and (*b*) pressure field ($\bar{p} \equiv p/\frac{1}{2}\rho w_p^2$) at a Taylor number of 45.

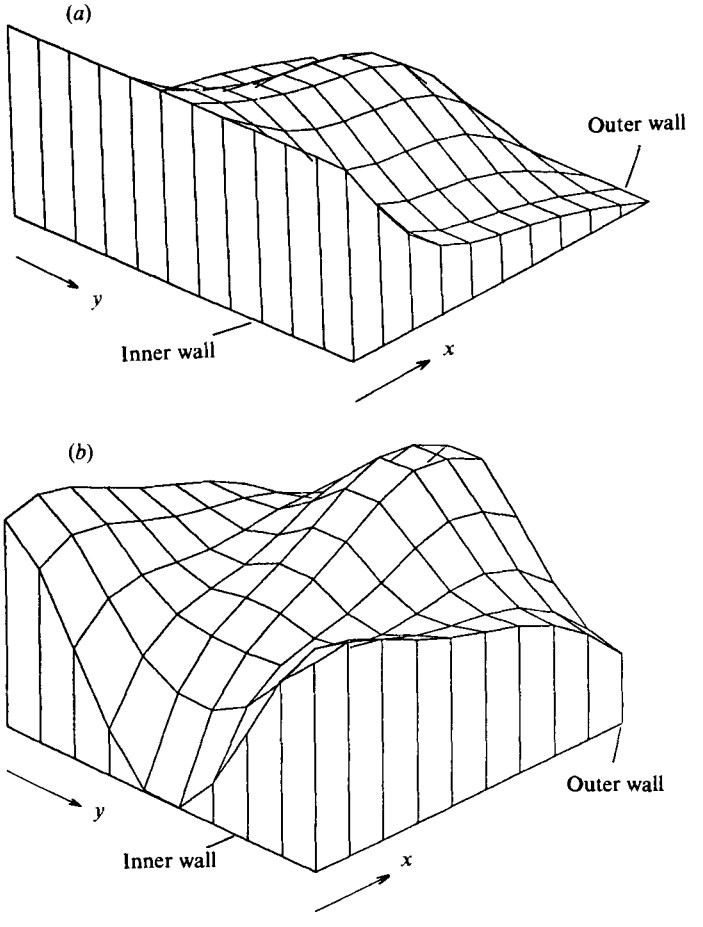

FIGURE 7. (*a*) Circumferential velocity ($\bar{w} = w/w_p$) distribution and (*b*) pressure field ($p \equiv p/\frac{1}{2}\rho w_p^2$) at a Taylor number of 55.

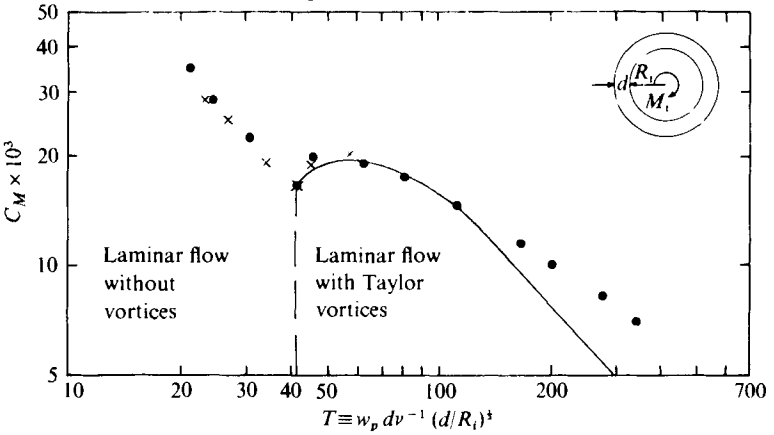

FIGURE 8. Comparison of predicted torque coefficient for inner cylinder ($C_M \equiv M_i/\frac{1}{2}\rho w_p^2 \pi R_i^2 h$) with measurements of Taylor (1936) and with prediction of Stuart (1958); $d/R_i = 0{\cdot}028$. ×, present numerical results; ●, Taylor's measurements; ——, Stuart's prediction.

that these are of an elliptic character, i.e. exhibit pressure-borne upstream influences of downstream events. In any case computations would have to extend over many cells and so would be either very expensive or rather inaccurate.

5. Conclusions

The finite-difference method of Patankar & Spalding has been successfully applied to predict the development of Taylor vortices in flow between concentric rotating cylinders. The predictions show physical realism and exhibit satisfactory agreement with experimental results. Further tasks are the following:

(i) Extension of the method to study the heat-transfer characteristics of such flows.

(ii) Application of the method to other vortex flows, e.g. Görtler vortices in the boundary layer on a concave wall.

This work forms a part of the research sponsored by the Science Research Council under Grant number B/RG/6848/7. The computer program was lent by CHAM Limited. Thanks are due to Colleen I. King and Christine MacKenzie for preparation of the typescript.

REFERENCES

COLES, D. 1965 *J. Fluid Mech.* **22**, 385.

COUETTE, M. 1890 *Ann. Chim. Phys.* (6), **21**, 433.

DAVEY, A. 1962 *J. Fluid Mech.* **14**, 336.

DIPRIMA, R. C. & STUART, J. T. 1972 *J. Fluid Mech.* **54**, 393.

DIPRIMA, R. C. & STUART, J. T. 1975 *J. Fluid Mech.* **67**, 86.

MALLOCK, A. 1888 *Proc. Roy. Soc.* A **45**, 126.

MEYER, K. A. 1966 *Los Alamos Sci. Lab. Rep.* LA-3497.

PATANKAR, S. V. & SPALDING, D. B. 1972 *Int. J. Heat Mass Transfer* **15**, 1787.

RAYLEIGH, LORD 1916 *Proc. Roy. Soc.* A **93**, 148.

STUART, J. T. 1958 *J. Fluid Mech.* **4**, 1.

TAYLOR, G. I. 1923 *Phil. Trans.* A **223**, 289.

TAYLOR, G. I. 1935 *Proc. Roy. Soc.* A **151**, 494.

TAYLOR, G. I. 1936 *Proc. Roy. Soc.* A **157**, 546.